INTERNATIONAL JOURNAL OF NUMERICAL METHODS IN FLUIDS, VOL. 13, 655–666 (1991)

CALCULATING HYDRODYNAMICS PROBLEMS FOR A LIQUID FILM FLOWING RADIALLY ON A FLAT HORIZONTAL SURFACE

BOGDAN SIWOŃ AND MUSTAPHA ENNAOUI

Department of Chemical Engineering and Physical Chemistry, Technical University of Szczecin, Al. Piastów 42, 71-065 Szczecin, Poland

SUMMARY

A mathematical hydrodynamic model of a thin liquid film flowing radially on a flat horizontal surface has been elaborated. The model consisted of continuity and momentum equations which were resolved by means of the integral method. In fact, several versions of the model were examined; they differed mainly in film velocity distribution. The predictions of the different versions were then compared with liquid film thicknesses obtained from experimental investigation. The best version was applied in further calculations.

KEY WORDS Two-phase jet Gas–liquid spray Liquid film

1. INTRODUCTION

During the last 20 years several investigations on heat transfer between a gas–liquid spray and a surface have been performed. These examinations concerned mostly the two-phase, two-component flow directed at the side surface of a cylinder.[1–8] The results showed quite a large augmentation of heat transfer in the process as compared with one-phase (gas only) flow application. The heat transfer coefficient values after gas–liquid spray had been applied were approximately 5–25 times larger than for pure gas. These large values of heat transfer coefficient could be attained as a result of the formation of a thin liquid film flowing on the heat transfer surface with a velocity of up to about $1\ m\ s^{-1}$.

Two problems were encountered in the case when the cylinder side surface was used as the heat transfer surface for gas–liquid spray flow. First, the heat transfer surface was covered by liquid film to the extent of about 50% or less, which decreased the heat transfer coefficient in the process. Secondly, droplets bounced against the film surface, the heat transfer surface was missed by the droplets and there occurred splashes in the thin film layer. For the above reasons, some investigations with different surface shapes were performed.

Smith[9] examined heat transfer by directing an air–water spray flow onto an elliptical cylinder as well as onto blunt bodies of rectangular and semicircular cross-section. Aihara *et al.*[10] investigated the heat transfer between a gas–liquid spray and a wedge as well as the possibility of the application of air–water mist flow to cool semiconductors.[11] So far, however, no investigations on heat transfer by a gas–liquid mist jet impinging perpendicularly on a flat surface have been performed. As one could expect, the augmentation of heat transfer in this case would be dependent on the size of the heat transfer surface covered by the film. The behaviour and

0271–2091/91/150655–12$06.00

Received November 1989
Revised November 1990

properties of the liquid film in relation to the liquid and gas velocities in the gas–liquid spray have been examined first. It emerged from the observations that, with proper mass flow ratios of gas and liquid in the two-phase stream, there is a thin flowing liquid film formed on the heat transfer surface, covering quite a large part of this surface.

Initial analysis of the heat transfer from a thin liquid film flowing radially on a flat horizontal surface[12] showed possibilities of heat transfer intensification. A heat transfer mathematical model elaboration of the process requires analysis of the flowing liquid film hydrodynamics. In this paper several versions of a mathematical model of a liquid film flowing radially have been worked out. In order to verify the model and to choose the proper version, experimental investigations of the liquid film thickness were performed.

For thickness measurements of the thin flowing liquid film the electrochemical method was applied, which was particularly useful for liquid layers less than 20 μm thick with two-phase flows. The thin liquid film was produced by application of a pneumatic atomizer supplied by compressed air and a 0·3% KCl–water solution. A two-phase stream was directed vertically onto a radial horizontal surface of diameter 0·31 m. A more detailed description of the measurement apparatus and method is given in Reference 13.

2. ANALYSIS

Analysis of the hydrodynamics of a gas jet impacting perpendicularly on a flat surface shows that two regions can be distinguished on the surface: the impingement region and the wall stream region. In the impingement region there is a change of the flowing gas direction from vertical to horizontal (Figure 1). At the stagnation point there occurs the highest value of pressure in the y-direction. Subsequently, there is a considerable decrease of pressure with x increasing up to $x = R_g$. For $x \geqslant R_g$ there is a wall stream region in which gas in the layer near the wall flows in the x-direction and pressure is equal to the environmental pressure. Considering the behaviour of a gas–liquid spray directed perpendicularly onto a flat surface, one can suppose that the behaviour of the gas phase in this case will be similar to the case of pure gas only.

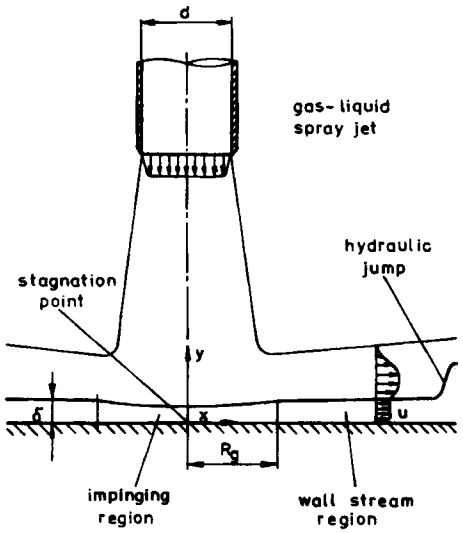

Figure 1. Sketch of a gas–liquid spray jet impinging perpendicularly on a flat surface

Taking into account investigations concerning the hydrodynamics and heat transfer of a gas jet impacting on a flat surface [14-18] and studies on the gas–liquid spray/surface system mentioned above, as well as our own observations, the following assumptions have been made.

1. The gas–liquid spray stream is directed vertically down onto the horizontal flat plate. The relation between the gas and liquid flow rates is such as to cover the whole surface or a part of the surface by a flowing thin liquid film.
2. Liquid droplets are uniformly distributed in the stream and impinge on the surface in the impingement region only.
3. All droplets are captured by the liquid film. The phenomena of bouncing and splashing are neglected.
4. The presence of droplets in the gas stream does not cause essential changes in its dynamics. The velocity and thickness of the gas boundary layer at the edge of the liquid film are similar to the case when a gas jet impinges on a flat surface.
5. The surface tension is neglected.

It has been additionally assumed that the film is smooth. Instantaneus waves and ripples are neglected since they have a secondary influence on the heat transfer between the surface and the liquid film.

The mathematical model consisted of the continuity and momentum equations in the following form:

continuity equation

$$\frac{\partial(xu)}{\partial x}+\frac{\partial(xw)}{\partial y}=A, \tag{1}$$

where

$$A=\frac{g_l x}{\pi R_g^2 \rho_l \delta} \quad \text{for the impingement region,}$$

$$A=0 \quad \text{for the wall stream region;}$$

momentum equation

$$\rho_l\left(u\frac{\partial u}{\partial x}+w\frac{\partial u}{\partial y}\right)=B, \tag{2}$$

where

$$B=-\frac{\partial P_g}{\partial x}-\eta_l\frac{\partial^2 u}{\partial y^2}+\frac{\partial \tau_\delta}{\partial y}+\frac{\partial P_x}{\partial y}\frac{\partial \delta}{\partial x} \quad \text{for the impingement region,}$$

$$B=-\eta_l\frac{\partial^2 u}{\partial y^2}+\frac{\partial \tau_\delta}{\partial y}+\frac{\partial P_x}{\partial y}\frac{\partial \delta}{\partial x} \quad \text{for the wall stream region.}$$

After integrating both sides of equations (1) and (2) from zero to δ resolving the integral $\int_0^\delta w(\mathrm{d}u/\mathrm{d}y)\mathrm{d}y$ by parts, the momentum equation can be presented as follows:

$$\frac{\mathrm{d}}{\mathrm{d}x}\int_0^\delta \frac{u^2}{2}\,\mathrm{d}y+\frac{1}{x^2}\frac{\mathrm{d}}{\mathrm{d}x}\int_0^\delta \frac{x^2u^2}{2}\,\mathrm{d}y+(uw)\Big|_0^\delta-\int_0^\delta A\frac{u}{x}\,\mathrm{d}y=\int_0^\delta \frac{B}{\rho_l}\,\mathrm{d}y. \tag{3}$$

For the thin liquid film the following equation can be written:

$$(uw)|_0^\delta = u_\delta^2 \frac{\mathrm{d}\delta}{\mathrm{d}x}. \tag{4}$$

Then the equations of continuity and momentum for the two regions appear in the following form

Impingement region

Continuity equation

$$\frac{\mathrm{d}}{\mathrm{d}x}\int_0^\delta xu\,\mathrm{d}y + xu_\delta \frac{\mathrm{d}\delta}{\mathrm{d}x} = \frac{g_1 x}{\pi R_g^2 \rho_1}; \tag{5}$$

momentum equation

$$\frac{\mathrm{d}}{\mathrm{d}x}\int_0^\delta \frac{u^2}{2}\,\mathrm{d}y + \frac{1}{x^2}\frac{\mathrm{d}}{\mathrm{d}x}\int_0^\delta \frac{x^2u^2}{2}\,\mathrm{d}y + u_\delta^2 \frac{\mathrm{d}\delta}{\mathrm{d}x} = \frac{g_1}{\pi R_g^2 \rho_1 \delta}\int_0^\delta u\,\mathrm{d}y + \frac{P_x}{\rho_1}\frac{\mathrm{d}\delta}{\mathrm{d}x} + \frac{\tau_\delta}{\rho_1} - \frac{\tau_p}{\rho_1} - \frac{\delta}{\rho_1}\frac{\mathrm{d}P_g}{\mathrm{d}x}; \tag{6}$$

Wall stream region

Continuity equation

$$\frac{\mathrm{d}}{\mathrm{d}x}\int_0^\delta xu\,\mathrm{d}y = -xu_\delta \frac{\mathrm{d}\delta}{\mathrm{d}x}, \tag{7}$$

momentum equation

$$\frac{\mathrm{d}}{\mathrm{d}x}\int_0^\delta \frac{u^2}{2}\,\mathrm{d}y + \frac{1}{x^2}\frac{\mathrm{d}}{\mathrm{d}x}\int_0^\delta \frac{x^2u^2}{2}\,\mathrm{d}y + u_\delta^2 \frac{\mathrm{d}\delta}{\mathrm{d}x} = \frac{P_x}{\rho_1}\frac{\mathrm{d}\delta}{\mathrm{d}x} + \frac{\tau_\delta}{\rho_1} - \frac{\tau_p}{\rho_1}; \tag{8}$$

and additionally

$$g_1 = 2\pi\rho_1 x \int_0^\delta u\,\mathrm{d}y. \tag{9}$$

The resolution method of the above equations depends upon the flow character. On the basis of the observations performed, it has not been absolutely clear whether the film is laminar or turbulent. Laminar flow of the liquid film could be expected in the wall stream region. It is quite certain that there should occur a turbulent flow in the impingement region.

Since the presence of neither of the flow types can be affirmed owing to the manner of our observations, the continuity and momentum equations are resolved for both laminar and turbulent flows. In order to state the character of the thin liquid film flow, experimental results were compared with calculations.

In order to resolve equations (5)–(9), the following velocity distributions in the y-direction had to be accepted.

Laminar flow

$$\frac{u}{u_\delta} = a_0 + a_1\varepsilon + a_2\varepsilon^2 + a_3\varepsilon^3, \quad \text{where } \varepsilon = y/\delta, \tag{10}$$

with the following boundary conditions:

	impingement region	wall stream region	
on the surface ($\varepsilon=0$)	$u=0,$	$u=0,$	(11)
	$\eta_l \frac{\partial^2 u}{\partial y^2}=\frac{\partial P_g}{\partial x},$	$\eta_l \frac{\partial^2 u}{\partial y^2}=0,$	(12)
on the film, edge ($\varepsilon=1$)	$u=u_\delta,$	$u=u_\delta,$	(13)
	$\tau_\delta=\eta_l \frac{\partial u}{\partial y},$	$\tau_\delta=\eta_l \frac{\partial u}{\partial y}.$	(14)

Application of the above boundary conditions allowed calculation of the constants a_0–a_3 in equation (10). Equations (5)–(9) were also resolved by application of the linear velocity distribution. In this case the right-hand side of equation (10) reduces to the first two terms by application of boundary conditions (11) and (13).

Turbulent flow

$$\frac{u}{u_\delta}=\varepsilon^{1/7}. \tag{15}$$

Substitution of the respective velocity distributions in equations (5)–(9) enabled us to obtain particular versions of the model: ordinary differential equations,

$$\frac{\mathrm{d}\delta}{\mathrm{d}x}=f(\delta, x, \tau_\delta, \tau_p, P_g, P_x); \tag{16}$$

or a system of two equations in the form

$$\frac{\mathrm{d}\delta}{\mathrm{d}x}=f(\delta, u_\delta, x, \tau_\delta, \tau_p, P_g, P_x), \tag{17}$$

$$\frac{\mathrm{d}u_\delta}{\mathrm{d}x}=f(\delta, u_\delta, x, \tau_\delta, \tau_p, P_g, P_x). \tag{18}$$

Formulae for calculation of the parameters τ_δ, τ_p, P_g, P_x and R_g are given in Appendix I. These formulae were received mainly in the empirical way for the impinging gas jet process and are readily available in the literature.

3. METHOD OF CALCULATIONS

The calculations were conducted by means of the fourth-order Runge–Kutta method in its basic version (see Reference 19, Chap. 5.4, p. 357) with automatic choice of integration step. For $x=0$ the right hand sides of most of the differential equations were equal to zero. It was difficult to derive initial conditions and therefore the calculations were begun with $x=0{\cdot}00001$ m, omitting the derivatives. These simplified equations were resolved by means of the Newton method and the results obtained were used as initial conditions for the first integration step of the full differential equations (16)–(18). The Runge–Kutta method was very stable for the equations in all the model versions.

4. RESULTS OF CALCULATIONS

The first goal of the calculations was to prove the influence of the dynamic pressure P_x and the velocity component in the y-direction, w, on the calculated results in comparison with the experimental results.

The occurrence of the dynamic pressure P_x in equations (6) and (8) was questioned because the influence of P_x had already been included in the shear stress τ_δ. However, the equations for τ_δ found in the literature concern a flat, smooth surface and the thickness of the liquid film changes; thus including the element

$$\frac{P_x}{\rho_l}\frac{\mathrm{d}\delta}{\mathrm{d}x} \tag{19}$$

in the momentum equations seemed to be justified.

The calculation results confirmed the above assumptions; however the influence of P_x on the results varied depending on the process parameters and the model version. A comparison of the liquid film thickness distributions along co-ordinate x with and without pressure P_x taken into account is shown in Figure 2. From the curve shape it appears that for the lower value of air flow

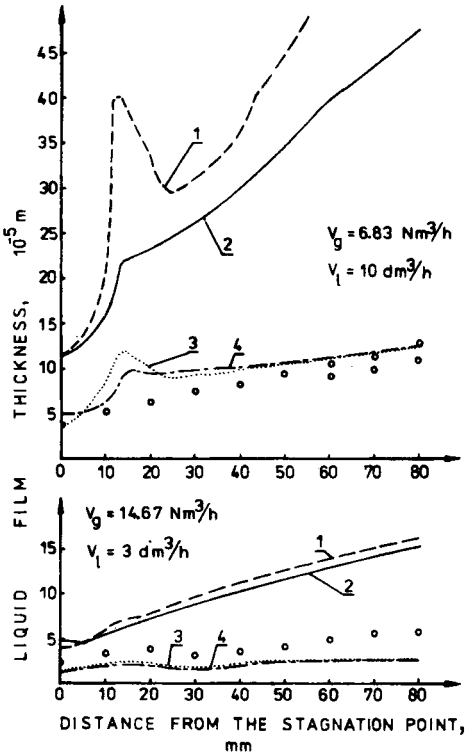

Figure 2. Distribution of liquid film thickness versus x-co-ordinate:
O, experimental points;
1, linear velocity distribution with P_x omitted;
2, linear velocity distribution with P_x included;
3, exponential velocity distribution with P_x omitted;
4, exponential velocity distribution with P_x included

rate ($V_g = 6{\cdot}83\ \mathrm{Nm^3\,h^{-1}} \equiv 0{\cdot}00246\ \mathrm{kg\,s^{-1}}$) and a linear velocity distribution omitting P_x in the model, the calculation results diverge from the experimental points. The curve obtained for the linear model with P_x included comes closer to the experimental results but the experimental points are still distinctly lower. For the exponential velocity distribution the influence of P_x is smaller, although it does seem to be advantageous if the dynamic pressure P_x is taken into account in the momentum equation.

For higher values of the air flow rate ($V_g = 14{\cdot}67\ \mathrm{Nm^3\,h^{-1}} \equiv 0{\cdot}00528\ \mathrm{kg\,s^{-1}}$) the influence of P_x on the liquid film thickness can be neglected in both the linear and exponential velocity distribution models. Generally, the influence of the dynamic pressure is visibly distinct for some ranges of flow parameters and its omission can cause significant errors.

The importance of the velocity component w in the y-direction is illustrated in Figure 3. In many works concerning liquid film flow the momentum equation includes only the velocity component u in the x-direction, whereas examination of the importance of w seems to be valid for further calculations. Both diagrams in Figure 3 show that there is a distinct difference between the curves obtained with and without the vertical velocity w in the impingement region taken into

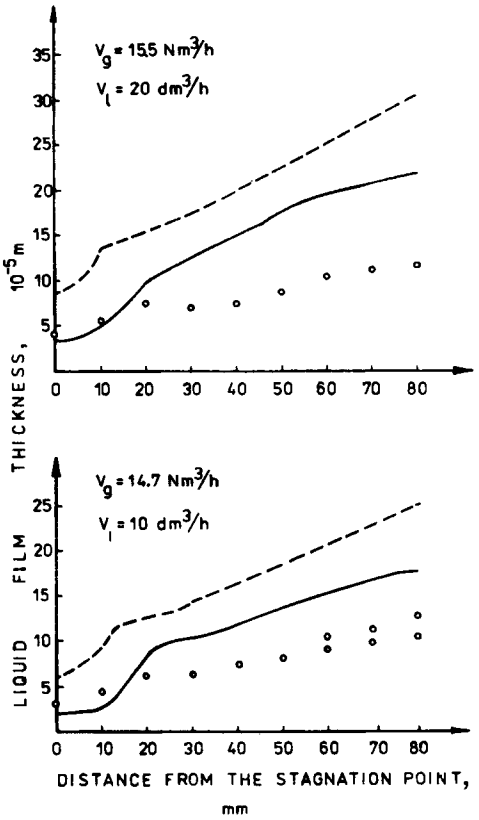

Figure 3. Liquid film thickness distributions calculated from the models with and without velocity component in y-direction:

O, experimental points;
——, model with velocity components in y-direction;
– – –, model without velocity component in y-direction

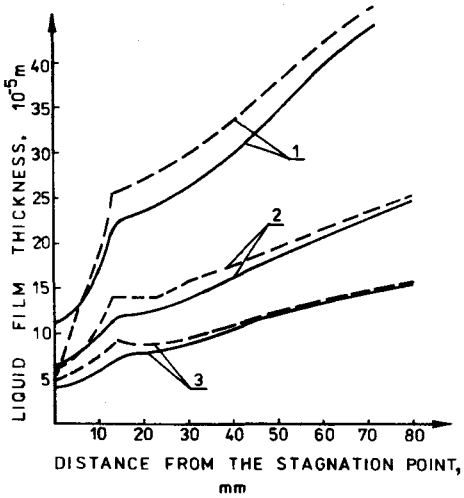

Figure 4. Comparison between results calculated from models with third-order polynomial and linear velocity distributions:

---, model with third-order polynomial velocity distribution;
——, model with linear velocity distribution;
1, $V_g = 6{\cdot}83\ \mathrm{nm^3\,h^{-1}}$, $V_l = 10\ \mathrm{dm^3\,h^{-1}}$;
2, $V_g = 14{\cdot}67\ \mathrm{nm^3\,h^{-1}}$, $V_l = 10\ \mathrm{dm^3\,h^{-1}}$;
3, $V_g = 24{\cdot}63\ \mathrm{nm^3\,h^{-1}}$, $V_l = 10\ \mathrm{dm^3\,h^{-1}}$

account. In the wall stream region both curves run closer to each other. In the impingement region the curves obtained with w taken into account agree well with the experimental points. In the wall stream region bigger distinctions are observed. This might be because the curves were calculated for a different type of flow than that in the present experiments. The results presented as four curves in Figure 4 were calculated for a linear velocity distribution in the y-direction (laminar flow). Similar calculations for an exponential velocity distribution (turbulent flow) gave results which did not differ much from each other. For this reason they are not presented here.

Generally, the mathematical model including both velocity components gives more complicated shapes of the momentum equations but the calculation results differ from each other for linear the velocity distribution.

When the continuity and momentum equations are resolved by means of the integral method, calculating the velocity distribution is an important problem. Equations (5)–(9) were resolved by application of the following distributions: linear, third-order polynomial and exponential (characteristic of turbulent flow). A comparison of the calculation results for the linear and third-order polynomial distributions has been shown in Figure 4. It is seen that the curves differ more for the smaller air flow rate. Generally, however, differences between the location and shape of the curves can be ignored.

A comparison of experimental liquid film thicknesses with calculation results for different velocity distributions in the y-direction was given in Figure 2. The diagram shows that the best agreement between measurement points and calculation results is achieved for an exponential velocity distribution (turbulent flow). This observation is confirmed in Figure 5, where a comparison between random results of measurements and results calculated from the mathematical model with an exponential velocity distribution is shown.

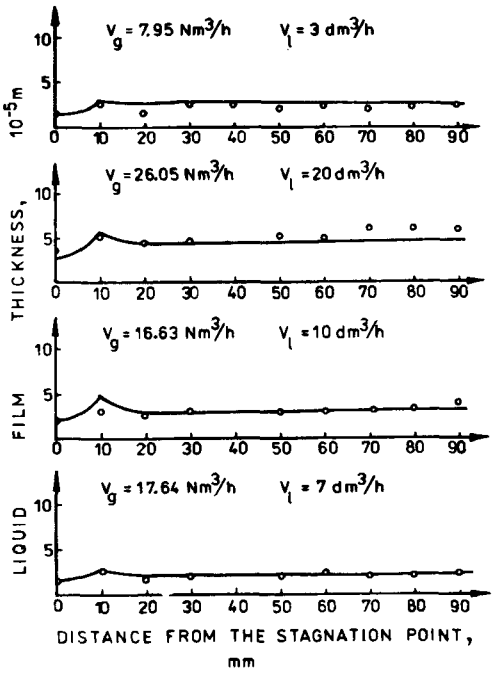

Figure 5. Comparison between curves obtained from model with exponential velocity distribution and experimental points

It can be seen that some disagreements observed for $x > 50$ mm (Figure 2) are caused by the occurrence of a hydraulic jump, which forms for smaller values of the air flow rate at a certain distance from the stagnation point and which was not considered in the analysis presented here.

5. CONCLUSIONS

From the comparison of the calculation results with the experimental data, the following conclusions can be drawn.

1. Including the dynamic pressure P_x of the gas in the momentum equation improves the agreement between the mathematical model and the experimental results, although in certain ranges of the process parameters its influence can be neglected.
2. Resolution of the continuity and momentum equations in the full form, i.e. taking into account the vertical component of liquid film velocity, for the linear velocity distribution seems to be more adequate than for the simplified version (with omission of the vertical component of film velocity). This conclusion could not be proved experimentally. Resolution of the continuity and momentum equations in the full form for the exponential velocity distribution gave results quite similar to the results when the simplified version was applied.
3. Application of the velocity distribution as a third-order polynomial produces a more complicated shape of equations, in comparison to the linear distribution, but the results of the calculations differ little from each other.

4. Application of the exponential distribution with a power of 1/7 (typical for turbulent flow) in the continuity and momentum equations gives good agreement between experimental and calculated results in both the impingement and wall stream regions.

APPENDIX I

The radius of the impingement region has been calculated from an equation given by Schrader:[18]

$$R_g = 1{\cdot}09(d/H)^{0{\cdot}034}d. \tag{20}$$

The external shear stress caused by flowing gas can be calculated, irrespective of the character of the gas flow, from the equation

$$\tau_\delta = 0{\cdot}00833\,\rho_g w_m^2 \left(\frac{\eta_g}{\rho_g w_m \vartheta}\right)^{2/13}, \tag{21}$$

where the maximum velocity of the gas in the x-direction in the impingement region is expressed according to the formula[18]

$$w_m = w_d\left(1{\cdot}04 - 0{\cdot}034\frac{H}{d}\right)\frac{x}{d} = A w_d \frac{x}{d}. \tag{22}$$

The thickness of the gas boundary layer, ϑ, is constant[18] and expressed by the equation (14)

$$\vartheta = 1{\cdot}83 R_g Re_d^{-0{\cdot}5}\left(\frac{R_g}{d}\right)^{-0{\cdot}5} \tag{23}$$

The dynamic pressure has been calculated from the equation

$$P_x = \frac{w_m^2 \rho_g}{2} = 0{\cdot}5\left(A w_d \frac{x}{d}\right)^2 \rho_g. \tag{24}$$

The pressure distribution in the impingement region has been given by Dawson and Trass:[15]

$$\frac{P_g}{P_{g,0}} = \left[1 - \left(\frac{x}{R_g}\right)^2\right]^4, \tag{25}$$

where the maximal pressure in the stagnation point is

$$P_{g,0} = 0{\cdot}5 w_d^2 \rho_g \qquad \text{for } H/d < 4,$$
$$P_{g,0} = 8 w_d^2 d^2 \rho_g / H^2 \qquad \text{for } H/d \geqslant 4.$$

The maximal velocity of the gas near the surface in the wall stream region has been given by Schrader:[18]

$$w_m = w_d\left[\frac{K_1}{1 + 0{\cdot}18(H/d - 1{\cdot}2)} + K_2\left(\frac{H}{d} - 1{\cdot}2\right)\left(\frac{x}{R_g} - 1\right)^{1/3}\right]\left(\frac{x}{R_g}\right)^{-1{\cdot}17}, \tag{26}$$

where $K_1 = 1{\cdot}1$, $K_2 = 0{\cdot}27$ for $H/d \leqslant 4{\cdot}7$ and $K_1 = 1{\cdot}45$, $K_2 = 0{\cdot}09$ for $4{\cdot}7 < H/d < 10$. The gas boundary layer thickness can be calculated from the equation[15]

$$\vartheta = 1{\cdot}83 x Re_d^{-0{\cdot}5}\left(\frac{x}{d}\right)^{-0{\cdot}5} \quad \text{for } H/d \leqslant 6{\cdot}2. \tag{27}$$

The surface shear stress in the turbulent liquid film has been calculated according to the Blasius equation:

$$\tau_p = 0{\cdot}0225\rho_l u_\delta^2 \left(\frac{\eta_l}{\rho_l \delta u_\delta}\right)^{1/4}. \tag{28}$$

APPENDIX II: NOMENCLATURE

d	diameter of nozzle (m)
g	mass flow rate ($kg\,h^{-1}$, $kg\,s^{-1}$)
H	distance between nozzle and surface (m)
P_g	pressure in y-direction (Pa)
P_x	pressure in x-direction (Pa)
R_g	radius of impingement region (m)
Re_d	Reynolds number in nozzle, $w_d d \rho_g / \eta_g$
u	velocity of liquid film in x-direction ($m\,s^{-1}$)
V	volume flow rate ($m^3\,s^{-1}$)
w	velocity of liquid film in y-direction ($m\,s^{-1}$)
w_d	velocity of gas in nozzle ($m\,s^{-1}$)
w_m	velocity of gas on liquid film surface in x-direction ($m\,s^{-1}$)
x, y	co-ordinates
δ	liquid film thickness (m)
ε	dimensionless co-ordinate, defined in equation (10)
η	dynamic viscosity ($kg\,m^{-1}\,s^{-1}$)
ϑ	thickness of gas boundary layer (m)
ρ	density ($kg\,m^{-3}$)
τ	shear stress (Nm^{-2})

Subscripts

g	gas
l	liquid
p	at surface
0	at stagnation point
δ	at edge of liquid film

REFERENCES

1. I. C. Finnlay, 'An analysis of heat transfer during flow of an air/water mist across a heated cylinder', *Can. J. Chem. Eng.*, **49**, 333–339 (1971).
2. J. W. Hodgson, R. T. Saterbak and J. E. Sunderland, 'An experimental investigation of heat transfer from a spray cooled isothermal cylinder', *Trans. ASME, Ser. C*, **90**, 457–463 (1968).
3. J. W. Hodgson and J. E. Sunderland, 'Heat transfer from a spray-cooled isothermal cylinder', *Ind. Eng. Chem. Fund.*, **7**, 567–572 (1968).
4. R. L. Mednick and C. P. Colver, 'Heat transfer from a cylinder in an air–water spray flow stream', *AIChE J.*, **15**, 357–362 (1969).
5. M. Pawłowski and B. Siwoń, 'Heat transfer from a cylinder in a gas–liquid spray flow stream', *Proc. 7th Int. Heat Transfer Conf., Vol. 5*, Munich, 1982, Hemisphere Publ. Corp., Washington–New York–London, 1982, pp. 349–353.
6. M. Pawłowski and B. Siwoń, 'Investigations of heat transfer between gas containing suspended liquid droplets and a cylinder', *Inz. Chem. Proc.*, **4**, 529–544 (1983) (in Polish).
7. M. Pawłowski and B. Siwoń, 'Calculating liquid droplets settling on a cylinder in gas–liquid spray flow', *Int. J. Heat Fluid Flow*, **5**, 179–184 (1984).

8. D. S. Wilson and A. F. Jones, 'Heat transfer from a spray-cooled cylinder', *Ind. Eng. Chem. Fund.*, **17**, 183–189 (1978).
9. D. C. Smith, 'Investigation of heat transfer from a heated blunt body in two-phase air–water spray flow', *MS Thesis*, Air University US Air Force, School of Engineering, Ohio, 1968.
10. T. Aihara, M. Taga and T. Haraguchi, 'Heat transfer from a uniform heat flux wedge in air–water mist flow', *Int. J. Heat Mass Transfer*, **22**, 51–60 (1979).
11. T. Aihara and R. Saga, 'Performance of a compact cooling unit utilizing air–water mist flow', *Trans. ASME, J. Heat Transfer*, **105**, 18–24 (1983).
12. B. Siwoń and M. Wiśniewski, 'Heat transfer by directing gas–liquid spray perpendicularly on a flat surface', *Proc. 8th Int. Heat Transfer Conf., Vol. 3*, San Francisco, 1986, Hemisphere Publ. Corp., New York, 1986, pp. 1237–1242.
13. B. Siwoń, 'The behaviour of a liquid film while gas–liquid spray is directed onto a flat surface', *Proc. 2nd Int. Symp. FLUCOME*, Sheffield, 1988, pp. 535–539.
14. P. M. Brdlik and V. K. Savin, 'Teploobmen v okrestnosti kritičeskoj točki pri osesimetričnom strujnom obtekanii ploskich poverchnostej raspolozennych normalno k potoku', *Inz. Fiz. Zh.*, **10**, 423–428 (1966).
15. D. A. Dawson and O. Trass, 'Mass transfer in a turbulent radial wall jet', *Can. J. Chem. Eng.*, **44**, 121–129 (1966).
16. M. Pawłowski and E. Suszek, 'Heat transfer by perpendicular impact of air jet on a flat surface', *Inz. Chem. Proc.*, **5**, 81–94 (1984) (in Polish).
17. V. K. Savin, 'Issledovanije gidrodinamiki v pristennom pograničnom sloje polugraničenoj strui', *Inz. Fiz. Zh.*, **17**, 733–736 (1969).
18. M. Schrader, 'Trocknung feuchter Oberflächen mittels warmluftstrahlen Strömungsforgänge und Stoffübertragung', *VDI Forschungsheft*, **27**, 486 (1961).
19. C. F. Gerald and P. O. Wheatley, *Applied Numerical Analysis*, 4th edn, Addison-Wesley, Reading, Massachusetts, 1989.
20. K. Hishida, M. Maeda and S. Ikai, 'Heat transfer from a flat plate in two-component mist flow', *Trans. ASME, J. Heat Transfer*, **102**, 513–518 (1980).
21. K. Hishida, M. Maeda and S. Ikai, 'Heat transfer in two-component mist flow. Boundary layer structure on an isothermal plate', *Proc. 7th Int. Heat Transfer Conf., Vol. 5*, Munich, 1982, Hemisphere Publ. Corp., Washington–New York–London, 1982, pp. 301–306.
22. M. Pawłowski and B. Siwoń, 'Heat transfer between gas–liquid spray stream flowing perpendicularly to the row of the cylinders', *Wärme Stoffübertr.*, **22**, 97–109 (1988).